



HAL
open science

Impact on peel strength, tensile strength and shear viscosity of the addition of functionalized low density polyethylene to a thermoplastic polyurethane sheet calendered on a polyester fabric

Pierre-Baptiste Jacquot, Didier Perrin, Benjamin Gallard, Romain Léger,
Patrick Ienny

► To cite this version:

Pierre-Baptiste Jacquot, Didier Perrin, Benjamin Gallard, Romain Léger, Patrick Ienny. Impact on peel strength, tensile strength and shear viscosity of the addition of functionalized low density polyethylene to a thermoplastic polyurethane sheet calendered on a polyester fabric. *Journal of Industrial Textiles*, 2017, 10.1177/1528083716686853 . hal-01772588

HAL Id: hal-01772588

<https://hal.science/hal-01772588>

Submitted on 20 Apr 2018

HAL is a multi-disciplinary open access archive for the deposit and dissemination of scientific research documents, whether they are published or not. The documents may come from teaching and research institutions in France or abroad, or from public or private research centers.

L'archive ouverte pluridisciplinaire **HAL**, est destinée au dépôt et à la diffusion de documents scientifiques de niveau recherche, publiés ou non, émanant des établissements d'enseignement et de recherche français ou étrangers, des laboratoires publics ou privés.

Impact on peel strength, tensile strength and shear viscosity of the addition of functionalized low density polyethylene to a thermoplastic polyurethane sheet calendered on a polyester fabric

Pierre-Baptiste JACQUOT, Didier PERRIN¹, Benjamin GALLARD, Romain LÉGER, Patrick IENNY

Centre des Matériaux des Mines d'Alès (C2MA), Ecole des Mines d'Alès, (Institut Mines Telecom), 30319 Alès Cedex – France

This article has been first published online in Journal of Industrial Textiles in January 10, 2017.

<https://doi.org/10.1177/1528083716686853>

Abstract

Coated technical textiles are widely used for several industrial applications. Most of these coated fabrics are made with a polyester fabric and a PolyVinyl Chloride (PVC) coating but in order to reduce the environmental impact, the producers are willing to substitute PVC by thermoplastic polyurethane (TPU). However, a technological lock of the calendering of TPU on polyester fabric is the ability to get a good adhesion of the coating on the fabric. Producers could increase the temperatures of extrusion of the coating but TPU have a short range of extrusion temperatures making it difficult to extrude. One solution is to make a blend with another polymer which has a higher extrusion temperature range. In the present work, the studies of the addition of Low Density PolyEthylene (LDPE) and Linear Low Density PolyEthylene grafted Maleic Anhydride (LLDPE-g-Ma) in polyurethane coating on the tensile strength of the sheet and on the peel strength with a polyester fabric have been studied as well as the influence of the extrusion temperature. SEM observations, FTIR spectrums and viscosity measurements have been performed to understand the behavior of the different blends. Results show that extrusion temperature and penetration depth of the coating in the fabric have a positive influence on the peel strength.

Keywords

Polyurethane, Fabric, Peel strength, Calendering, Polymer

¹ Corresponding author : didier.perrin@mines-ales.fr, +33466785369

1.Introduction

Coated technical textiles are widely used for several applications like sails, big tops, paragliders or inflatable boats and the demand is still on the rise. These very light technical textiles are usually manufactured with a polyester fabric and a PolyVinyl Chloride (PVC) matrix. However, environmental constraints force the manufacturers to find a substitute material for the PVC which is harmful and difficult to recycle (1). Thermoplastic PolyUrethane (TPU) is a good substitute material for the PVC. Depending on its formulation and the components, TPU can have good properties (2) such as UV resistance (3) (4), abrasion resistance (5), solvent resistance (6), tensile strength (7) or high elongation (8). These properties make TPU an attractive material for coated textiles (9) or for leather like products (10). These TPU coated textiles are used for inflatable boats, flexible tanks or more technical applications like Lighter-Than-Air systems for high altitude applications (11).

Despite all these good properties, there is still a technological lock. Some industrials report that they are recalcitrant to use polyurethane sheets for coated textile because of very low peel strength of the sheet on the polyester fabric after calendering. To the best of our knowledge, industrials are more willing to use other processes like knife-over-roll coating or air-knife coating. These two methods are especially used for tightly fabrics where a low thickness of polyurethane is required like waterproof garments or materials for small inflatable boats (12) (13). But if a more important thickness is needed, these methods are quite difficult to use and manufacturers do not have any other choice than using calender coating or rotary-screen coating which are also cheaper than the others (12). To use both mentioned processes, they have to make special surface treatments on the fabrics. Six theories have been proposed to explain the different mechanism of adhesion: mechanical interlocking (14), wetting (15), diffusion (16), electrostatic (17), chemical (18) and weak boundary layer (19). All these theories show that the adhesion between two materials is linked with the interface as outlined by Mittal (20). Further studies explain that the quality of adhesion between the fabric and the

matrix is a key parameter to obtain good mechanical performance of the composite (21). As a consequence, several treatments have been developed to enhance the quality of the interface. Previous researches used different treatments for the fabric such as atmospheric air or corona plasma treatments to modify the surface energy of the fabric and increase the adhesion of the coating. For example, Leroux et al. showed that the adhesion of a silicon resin on a polyester fabric after atmospheric air plasma treatment has been multiplied by two (22). There are numerous other papers that deal with plasma treatment and their influence on the hydrophilicity increase of the treated fabric (23) (24) (25) (26) (27) (28) (29). However Novak et al. showed that the shelf-life of these treatments for a polypropylene material with polyvinyl acetate was only about 50 days due to the loss of the surface oxidation (30). Other research used corona treatments (31) (32) (33) or chemical treatments (34) (35) to increase the wettability of the fabrics.

One possibility is to increase the extrusion temperature in order to modify the viscosity and the surface energy. The problem is that TPU has a short range of extrusion temperatures and an increase of only 5°C can generate a drop in the viscosity of the polymer making it impossible to calender on a fabric. Hence we propose to make a blend with Low Density Polyethylene (LDPE) and Linear Low Density PolyEthylene grafted Maleic Anhydride (LLDPE-g-Ma). The aim of this blend is to extrude the sheet at higher temperatures in order to get a better adhesion with a polyester fabric.

Because of their high difference of polarities and their high interfacial tension, Polyurethane and Polyethylene are two immiscible materials. However, previous researches explain that it is possible to have a compatibility if the PE is grafted with maleic anhydride (36) (37) or secondary amine (37). These compatibilizers are capable to stay at the interface and entangling with both sides. The final material is then prepared by calendering the sheet of TPU/LDPE blend on a polyester fabric. According to the literature, there is no previous research about the influence of this blend on the plastic sheet adhesion on a polyester fabric.

However we can notice that Jie Song et al. show that the adhesion of a polyurethane paint was greater on a polyolefin/TPU blend substrate than on a simple PO substrate (38).

This paper proposes a new solution to enhance the adhesion of the sheet on the fabric. It suggests a modification of the plastic sheet that is extruded before being calendered. Thanks to an experimental design, the influences of extrusion temperature as well as the influence of LDPE and PE-g-Ma percentage in the blend on the peel strength and the mechanical performance of the film is analyzed. The value of the adhesion of the sheet on the fabric is the main proof of the influence of the blend. The sheet viscosity, the miscibility of the LDPE and PE-g-Ma in the TPU, the penetration depth of the coating in the yarns of the fabrics and the FTIR analysis are used to analyze and explain the results of the adhesion.

2. Materials and Methods

2.1 Materials Characterization

2.1.1 The coating

As presented previously, several blends have been realized with Low Density Polyethylene (LDPE), Thermoplastic PolyUrethane (TPU) and Linear Low Density Polyethylene Grafted Maleic Anhydride (LLDPE-g-Ma). References and properties of LDPE, LLDPE-g-Ma and TPU are gathered in Table I and Table II.

Table I: Main properties of LDPE (Low Density Polyethylene) and LLDPE-g-Ma (Linear Low Density Polyethylene grafted maleic anhydride).

	LDPE LD 171 BA	LLDPE-g-Ma OREVAC OE825
Manufacturer	EXXON MOBILE®	OREVAC® by ARKEMA
Density	0.929g/cm ³	0.913g/cm ³
Melt Index (190°C/2.16kg)	0.55g/10min	3g/10min
Peak Melting Temperature	114°C	118°C
Additives	no	Maleic anhydride

Table II: Main properties of TPU.

IROGRAN A 90 P 5055 DP	
Manufacturer	HUNTSMAN®
Isocyanate	Aromatic
Alcohol	Polyether
Density	0.7g/cm ³
Melt Index (190°C/10kg)	42g/10min
Peak Melting Temperature	113°C
Additives	no
Recommended injection temperature	190°C-200°C

2.1.2 The fabric

The coating has been calendered on the polyester fabric described in Table III.

Table III: Main properties of the fabric.

Composition	Polyester
Weaving	Plain
Additives on the surface	No
Number of yarns per cm : weft	18
Number of yarns per cm: warp	18
Thickness (µm)	170
Fabric weight (g/m²)	105
Number of filaments per yarn	48
Filament diameter (µm)	23
Yarn count (g/km)	28
Mechanical properties: weft (daN/5cm)	155
Mechanical properties: warp (daN/5cm)	155

This fabric (Figure 1) has been woven without the use of any additives like sizings on the surface of the yarns to avoid a decrease of the wetting capacity (39).

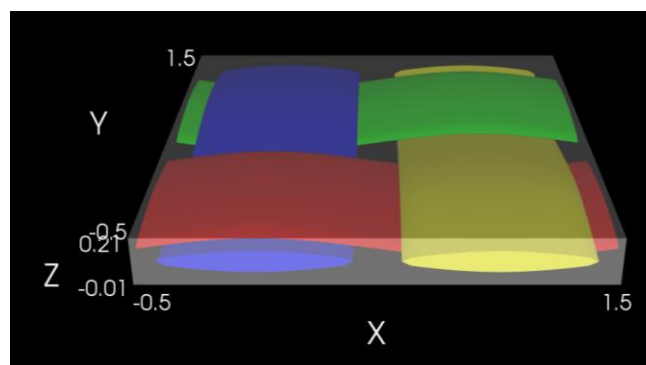


Figure 1: Modelization with a TexGen© software of the plain fabric used in the study.

2.2 Experiments Methods

2.2.1 Experimental design

2.2.1.1 Introduction to experimental designs

An experimental design has been used to minimize the number of experiments. In a first part, the experiments have been conducted with only *Temperature* and *LDPE amount* parameters. Then the blends giving the best compromise between adhesion and mechanical characterization have been adapted by adding of LLDPE-g-Ma.

2.2.1.2 Central Composite Design (CCD)

To define the optimum settings of these two factors level which can significantly influence the adhesion and mechanical characterization, a Central Composite Design (CCD) was applied in the experimental domain presented in Table IV (40) (41) (42).

Table IV: Composite design.

Variable	Factor	Unit	Center	Step of variation
X_T	Temperature	°C	192,50	12,38
X_{PE}	PE amount	wt%	50,00	35,36

Actually, the most popular response surface method based on a rotatable central composite design with five levels and two factors was applied to investigate the influence of process factors on multiple responses including: adhesion (Y1) and mechanical characterization (Y2).

In CCD designs, all process variables are studied in five levels ($-a$, -1 , 0 , $+1$, $+a$); each of these values is a code for an original variable value. Coding the variable levels is a simple linear transformation of the original measurement scale so that the highest value of the original variable becomes ($+1$) and the lowest value becomes (-1). The average of these two values is assigned to (0) while the values of $-a$ and $+a$ are applied to find the minimum and the maximum values. The a values depend on the number of variables studied (2 in our case) and for two, three, and four variables, they are 1.41, 1.68, and 2.00, respectively. All design descriptions are in terms of coded values of the variables. The independent variables for this study and their related levels and codes are shown in Table V.

Table V: Original and coded values of the independent variables of the extraction process.

Independent variables	Symbols	Coded values				
		-1.41	-1	0	1	1.41
		Original values				
Temperature (°C)	T	175	180	192.5	205	210
PE amount (%)	PE	0	16.67	50	85.36	100

CCD's are designed to estimate the coefficients of a quadratic model. To get the best response surface, rotatable CCDs are commonly applied. Rotatability implies that the variation in the response prediction will be constant at a given distance from the center of the design. The design matrix for a rotatable CCD for 2 variables (each one evaluated at 5 levels), involves 9 design points or experiments with adding of 3 additional experiments called *check points* (runs nos. 10 to 12) in order to subsequently check the validity of the fitted models. After performing 12 different experiments, a quadratic model was fitted to the response data using Nemrodw 2015 software. The whole table data (Table VI) is presented in the part *Results*. The complete quadratic model for k variables contains $(k + 1)(k + 2)/2$ parameters and is given by:

$$Y = \beta_0 + \sum_i \beta_i X_i + \sum_{i < j} \sum_j \beta_{ij} X_i X_j + \sum_i \beta_{ii} X_i^2 \quad (1)$$

where the notation β_i is the coefficient of linear terms X_i , β_{ii} is the coefficient of quadratic terms X_i^2 , and β_{ij} is the coefficient of interaction terms $X_i X_j$. Each variable in the model has a coefficient. Numerical magnitude of the standardized model coefficients reveal their importance in the obtained model and the modeled response, accordingly (among standardized coefficients the larger values are more effective). Furthermore, negative coefficients represent inverse effect of the corresponding factor on the modeled response. In addition to a quadratic model, the model can also be displayed in three dimensions plots. The CCD outputs include contour and 3D response surface plots, which visualize the results of the experiment and enable the researcher to visually examine the relationships between the variables in the plot and the response.

A statistical test of the model fit is made by comparing the variance due to the lack of fit to the pure error variance using the F -test. The fitted model is considered adequate if the variance due to the lack of fit is not significantly different from the pure error variance (43) (44) (45). The adequacy of the model is further tested using three check points (43).

The search for experimental conditions which optimize the five responses simultaneously requires the use of the desirability function approach. The method consists in transforming the measured property of each response to a dimensionless desirability scale d_i defined as a partial desirability function. This makes possible the combination of the results obtained for properties measured on different scales. The scale of the desirability function ranges between $d = 0$, for a completely undesirable response, and $d = 1$, if the response is at the target value. Once the function d_i is defined for each of the responses of interest, an overall objective function (D), representing the global desirability function is calculated by determining the geometric mean of the individual desirabilities. Therefore, the function D over the experimental domain is calculated using Eq. (2) as follows (43) (45) (46):

$$D = \sqrt{d_1 \cdot d_2} \quad (2)$$

Taking into account all requirements for all responses, we can, thus, choose the conditions on the design variables that maximize D .

One can see that a high value of D is obtained only if all individual desirabilities d_i are high. The values of D computed from the observed responses allow us to locate optimal region.

2.2.2 Blend preparation

The LDPE/TPU blends have been prepared in two steps. First the pellets of TPU and LDPE (and/or LLDPE-g-Ma) have been well mixed in a container and then extrusion film experiments have been carried out using a single screw extruder with a Maddock mixer following.

2.2.3 Extrusion – calendering process

Extrusion has been performed with a laboratory-scale extruder Polylab system composed of a HAAKE RheoDrive4 motor coupled with a HAAKE Rheomex 19/25 OS single screw extruder with a Maddock mixer.

The system was piloted by PolySoft OS software to set and control temperature zones and screw speed. The extruder unit was equipped with a fish-tail designed die of 100mm wide and 450 μ m thick to process the molten polymer into a film. The extruder was connected to the air network which provides ambient temperature air to cool the hopper zone. The calendering was performed on only one face of the fabric using a 3-roll laboratory calender from THERMO SCIENTIFIC according to Figure 2. The rolls were 200mm wide and were cooled with a HAAKE Phoenix II P1 thermostat (THERMO SCIENTIFIC) with oil and regulation pump speed.

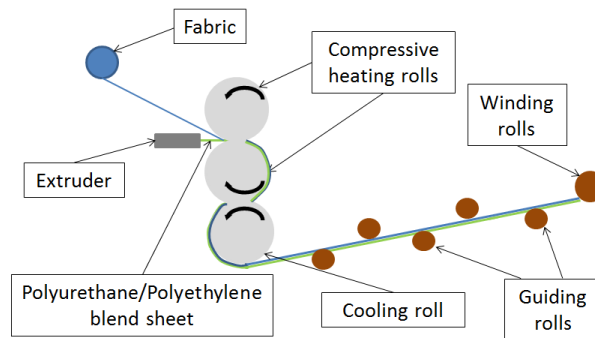


Figure 2: Scheme of the calendering process.

The Table VI collects all the process parameters for the extrusion-calendering.

Table VI: Process parameters.

Parameters	Value
Die gap	450 μ m
Die temperature	[174°C; 209°C] (+/-1°C) (see Erreur ! Source du renvoi introuvable.)
Extrusion speed	60 rpm
Calendering speed	6 rpm
Temperature of the thermoregulated rolls	40°C
Distance between the die and the rolls	20mm

In the purpose to have the ability to test the mechanical performance of the films that were calendered on the fabric, the same films were prepared with the same parameters but without fabric.

All prepared films parameters were summarized in Table VII. The experiments from 13 to 15 included grafted maleic anhydride. These experiments have been made according to the results from the experimental design (see Results).

The films produced had a thickness of 200 μ m corresponding to the gap between the compressive heating rolls of the 3-roll laboratory calender. This is the lower thickness that it was possible to obtain with the calender. This thickness has been chosen to get the lighter material as possible.

Table VII: Composition and extrusion temperatures of the different blends.

Sample number	1	2	3	4	5	6	7	8	9	10	11	12	13	14	15
Hopper zone	211	180	202	196	202	196	216	187	180	170	180	196	180	196	196
Zone 1	211	180	202	196	202	196	216	187	180	172	180	196	180	196	196
Zone 2	206	175	197	191	197	191	211	182	175	174	175	191	175	191	191
Die	199	174	196	190	196	190	210	181	174	175	174	190	174	190	190
% TPU	83.4	81	81	77.5	85	71	77.5	83.4	85	100	0	0	0	71	71
% LDPE	16.6	19	19	22.5	15	29	22.5	16.6	15	0	100	100	0	0	26
% PE-g-Ma	0	0	0	0	0	0	0	0	0	0	0	0	100	29	3

The different heating zones of the extruder are presented in the Figure 3 (47).

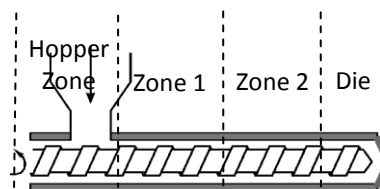


Figure 3: Scheme of the extruder and temperature zones (47).

2.2.4 Analysis of the Peel strength

The peel strength of the coating sheet on the fabric has been determined by a peel test carried out on a Zwick Z010 according to the standard NF EN ISO 2411. Samples were cut from the middle of the coated fabrics to avoid edge effects. The coating was first separated from the fabric using a tweezer and a cutting blade. The 50 mm width coating sheet and the fabric were clamped separately on the machine with a distance of 50 mm between grips (Figure 4). A crosshead speed of 100 mm/min and a 0.5 kN cell was chosen. During the test the force was recorded as a function of displacement thanks to TestXpert® II software (Zwick). Reported data are the average of five samples.

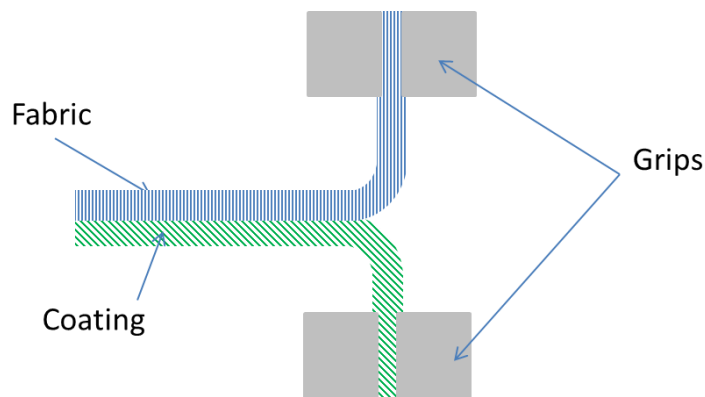


Figure 4: Scheme of the peel strength test according to standard NF EN ISO 2411

2.2.5 Analysis of the mechanical properties of the sheet

Tensile strength of blends sheets has been measured during a tensile test on a Zwick Z010 with a crosshead speed of 500 mm/min and a 0.5 kN cell. Strip-shaped samples were prepared with a cutting press. The length and width of samples is 40 mm and 10 mm respectively and the thickness is measured for each samples. The distance between grips is set at 40 mm to avoid slippage in the grips.

During the test, the force has been recorded as a function of the displacement thanks to TestXpert® II software (Zwick). Reported data are the average of 10 samples. The tensile strength was obtained by dividing the force applied at the breaking by the initial section of the sample.

2.2.6 Analysis of the shear viscosity of the blend

The dynamical rheological measurements have been performed on disks using a strain controlled rheometer ARES (TA Instrument) equipped with a 25 mm parallel plates geometry in continuous shear mode at the same temperatures than those used for the different calendering tests. According to prior experiments consisting in determining the linear viscoelastic domain for which the behavior of the polymer does not depend of the strain, the frequency sweep at strain was kept at $\epsilon=3\%$ and the pulsation ω was in the range of 0.1 to 100 rad/s. Nitrogen was used to decrease the ageing of blends. Disk samples of 1.8 mm thick and 25mm wide were prepared by injection. The gap was set at 1.5mm. The result is the average value of three samples.

2.2.7 Analysis of the coated textile sections and of the blends morphology

The section of the coated textile has been analyzed with a Scanning Electron Microscope using the detection of backscattered electrons and a magnification of x500.

The penetration of the coating on the fabric has been measured as following. Red arrows in Figure 5 indicate the depth of coating penetration:

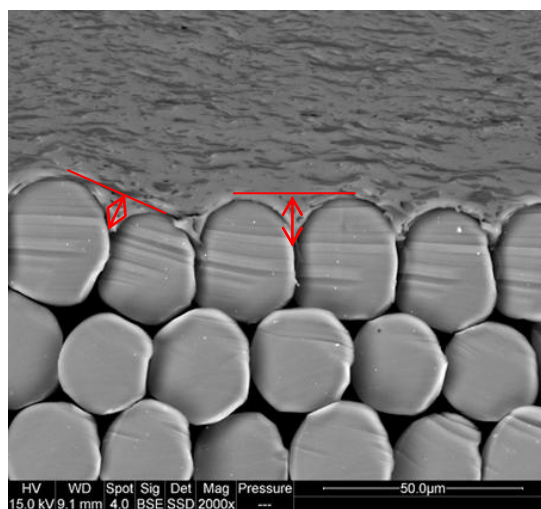


Figure 5: Measurement method of the coating penetration on the fabric.

The analysis of the compatibility between TPU and PE was realized by the observation of the presence of PE particles in TPU with the same Scanning Electron Microscope using the detection of backscattered electrons and a magnification off x1000. The morphology gave information about the compatibility between these two materials.

2.2.8 Analysis of the chemical composition

Infrared measurements at room temperature were performed on a Perkin–Elmer Spectrum One FT-IR (Fourier Transformed Infrared) Spectrometer with 32 scans and a resolution of 2 cm^{-1} in the absorption mode to determine the chemical composition of the different blends.

3. Results

3.1 Peel Strength of TPU/LDPE blends

According to Table VIII, peel strengths of neat TPU do not exceed 7N/50mm. For the blends given in the Table VIII, an increase between 200% can be highlighted for experiment number 9 (15% of LDPE and extrusion temperature 174°C) and 430% for experiments 4 and 6 (respectively 23% and 29% of LDPE and extrusion temperature 190°C). However neat LDPE (at both 174°C and 175°C) also exhibit a very low peel strength which means that the increase of the peel strength of the blends is not only due to the LDPE.

Table VIII: Peel strength of neat TPU, neat LDPE and TPU/LDPE blends.

Sample number	1	2	3	4	5	6	7	8	9	10	11	12
LDPE ratio	16.6	19	19	22.5	15	29	22.5	16.6	15	0	100	100
Die temperature ($^{\circ}\text{C}$)	199	174	196	190	196	190	210	181	174	175	174	190
Peel strength (N/50mm)	22.3	13	27.4	30	29.1	30	21.2	17	13	7	1.8	4.5
Standard deviation	2.14	0.53	2.8	1.61	2.62	2.06	2.7	0.3	0.78	0.31	0.22	0.46

For a same amount of LDPE, an increase of the extrusion temperature seems to increase the peel strength. For example, for a same amount of 19%wt of LDPE (samples 2 and 3) but different extrusion temperatures (respectively 174°C and 196°C), the peel strength is doubled (13.02N/50mm and 27.43N/50mm respectively). The same trend is observed with samples 1 and 8, while the opposite trend is observed with samples 4 and 7. This can be explained by the very high die temperature employed for sample 7 that may cause a degradation of the blend. This is further correlated to an important decrease of the tensile strength.

Conversely and for a same extrusion temperature the amount of LDPE seems to have slight influence on the peel strength. For example, experiments 2 and 9 have been both performed at 174°C with respectively 19%wt and 15%wt of LDPE but the peel strengths are nearly the same (respectively 13.02N/50mm and 13N/50mm). This observation is also true for experiments 4 and 6 and experiments 3 and 5.

3.2 Tensile strength of TPU/LDPE blends

Tensile strengths of the different blends are displayed in Table IX. Tensile strengths of neat TPU at 175°C is about 23 MPa while the tensile strength of neat LDPE depends of the process temperature (24.6MPa and 42.6 MPa for extrusion temperatures of, respectively, 174°C and 190°C. The difference can be due to the partial fusion of LDPE pellets at a temperature of 174°C while the fusion is complete at 190°C). Excepted for experiment 9, the tensile strength of all blends is lower than the tensile strength of neat TPU and neat LDPE which means that there is an incompatibility between TPU and LDPE (36) (37). For an extrusion temperature of 210°C, the film seems to be degraded. The corresponding tensile strength is only 11.6 MPa while it is more than 14 MPa for all other blends. It is important to note that the tensile strength of TPU/LDPE blends seems to depend on temperature. Indeed, except for experiment 3, an increase of the extrusion temperature leads to a decrease of the tensile strength.

Table IX: Tensile strength of neat TPU, neat LDPE and TPU/LDPE blends.

Sample number	1	2	3	4	5	6	7	8	9	10	11	12
Amount of LDPE (%)	16.6	19	19	22.5	15	29	22.5	16.6	15	0	100	100
Die temperature (°C)	199	174	196	190	196	190	210	181	174	175	174	190
Tensile strength (MPa)	14.3	22.5	17.9	13.9	17.8	18.6	11.6	18.7	25.5	23.1	24.6	42.6
Standard deviation	0.82	0.99	0.7	0.77	1.1	0.85	0.92	1.04	1.48	2.01	1.69	0.74

3.3 Analysis of Experimental design optimization

Table X shows 12 different experimental runs of CCD and the corresponding response data.

3.3.1 Model equations

Results of experiments of the CCD design are used to estimate the model coefficients (without using the check points). The fitted models expressed in coded variables are represented by Eqs. (3)– (4):

- Interfacial adhesion (Y1):

$$\hat{y}_1 = 28.44 - 0.97X_T - 5.82X_{PE} - 3.22X_TX_{PE} - 4.79X_T^2 - 8.11X_{PE}^2 \quad (3)$$

- Tensile strength (Y2):

$$\hat{y}_2 = 24.12 - 2.64X_T + 10.75X_{PE} + 7.33X_TX_{PE} - 0.13X_T^2 + 2.71X_{PE}^2 \quad (4)$$

Table X: CDD design matrix along with the experimental responses.

No	X ₁ : Temperature (°C)	Polyethylene amount (%)	Response Y1(interfacial adhesion) (N/50 mm)	Response Y2 (tensile strength) (MPa)
1	199	16.0	22.31	14.28
2	174	19.0	13.02	22.46
3	196	19.0	27.43	17.90
4	190	23.0	30.00	13.87
5	196	15.0	29.07	17.75
6	190	29.0	30.00	18.62
7	210	22.5	21.19	11.65
8	181	16.6	17.00	19.00
9	174	15.0	13.00	26.00
10	175	0.0	7.00	23.00
11	174	100.0	1.83	24.58
12	190	100.0	4.53	42.64

3.3.2 Statistical analysis and validation of the models

The analysis of variance for the fitted models showed that in all cases, the regression sum of squares was statistically significant (their p -value is less than 0.05) and the lack of fit is not significant (43) (46). Table XI illustrates the ANOVA corresponding to two responses namely *interfacial adhesion* (\hat{y}_1) and *tensile strength* (\hat{y}_2). In addition, Table XII shows the check point results used to validate the accuracy of the models.

Table XI: Analysis of the responses of the CCD design.

Source of variation	Sum of squares	df	Mean square	Ratio	Significance (p -value)
<i>(1) Interfacial adhesion</i>					
R²=0.958 & adj R²=0.924					
Regression	1.09.10 ³	5	2.19.10 ²	27.59	0.0453***
Residuals	4.76.10 ¹	6	7.94.10 ⁰		
Total	1.14.10 ³	11			
<i>(2) Tensile strength</i>					
R²=0.932 & adj R²=0.875					
Regression	6.76.10 ²	5	1.35.10 ²	16.39	0.193**
Residuals	4.95.10 ¹	6	8.24.10 ⁰		
Total	7.25.10 ²	11			

*significant at the level 95%; **significant at the level 99%; ***significant at the level 99.9%; (NS): non-significant at the level 95%.

Table XII: Numerical results for check points.

Ru n	Y_{exp}	Y_{calc}	$Y_{exp} - Y_{calc}$	dU	t -test
<i>(1) Interfacial adhesion</i>					
10	7.00	5.81	1.19	0.80	0.942
11	1.83	1.54	0.29	0.99	1.008
12	4.53	4.91	-0.38	0.98	-1.029
<i>(2) Tensile strength</i>					
10	23.00	24.99	-1.99	0.80	-1.557
11	24.58	24.99	0.41	0.99	-1.435
12	42.64	42.11	0.53	0.98	1.407

The measured values were very close to those calculated using the model equations. Indeed, the differences between calculated and measured responses were not statistically significant when using the t -test as shown in Table XII (equivalent Student values in function of both the response). It could be concluded that the second order models were adequate to describe the two response surfaces and could be used as prediction equations in the studied domain.

3.3.3 Interpretation of the response surface models

Following the validation of the model, the isoresponse curves were drawn for each response by plotting the response variation against both the factors. (Temperature in °C vs PE amount in wt %). **If zones of interest boundaries are set (according to the targets: adhesion and tensile strength), these curves are very useful.** Below are discussed the results corresponding to the two studied responses:

- *Interfacial adhesion* (\hat{y}_1): The examination of interfacial adhesion of TPU/LDPE mixture isoresponse curves (Figure 6) shows that the high values of T and PE give a negative effect on the response. The maximal interfacial adhesion 29.48 N/50 mm) is reached at a PE ratio in the range 38-39% and a mixture temperature of 192.5°C.
- *Tensile strength* (\hat{y}_2): The isoresponse curves in Figure 6 show that the tensile strength of the blends is almost the same for temperatures lower than 200°C and a PE amount of 50%. Actually, the range of \hat{y}_2 is between 19 and 22 N. Beyond this value, tensile strength sharply increases to reach 42N. In addition, the temperature has not an important effect on the response in the studied domain in contrast to the PE amount.

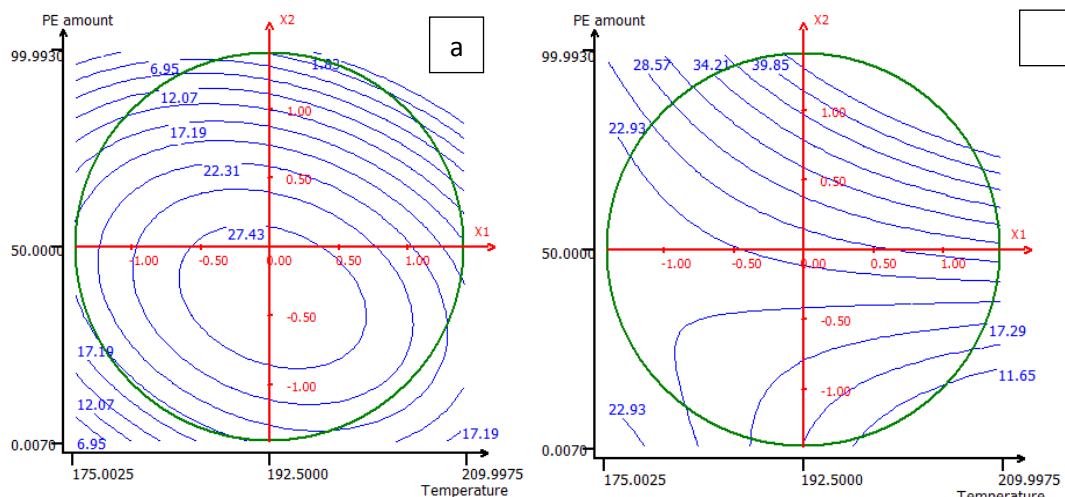


Figure 6: (a– b): Isoresponse curves in the plane: (a) Interfacial adhesion (Y1) and (b) Tensile strength (Y2).

The examination of all the results obtained by means of the isoresponse curves, allows us to deduce that it is not obvious how one can find experimental conditions that can optimize both

the responses simultaneously. The desirability functions allow to reach a compromise which can better satisfy conflicting objectives.

3.3.4 Optimization

The partial desirabilities of the two responses established based on the study of the behavior of some TPU/LDPE mixtures are shown in Figure 7. A target is fixed at 28 N / 50 mm and 25 MPa for the interfacial adhesion and tensile strength responses respectively. After calculation by the NEMRODW 2015 software, a three-dimensional plot of the global desirability function D can be represented as shown in Figure 8. We can note the rather flat area corresponding to the optimal conditions ($D=0.84$).

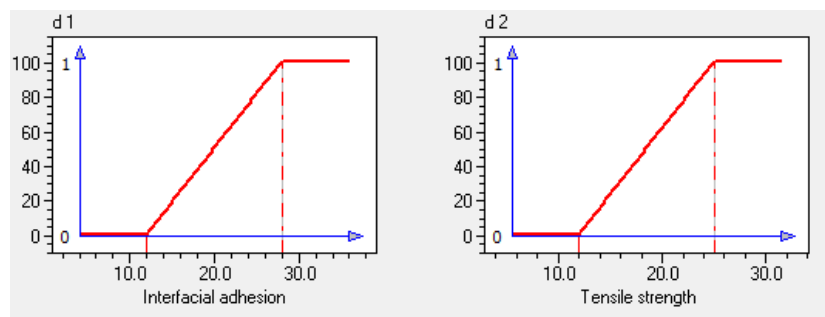


Figure 7: Individual desirability function of the responses (d1: Interfacial adhesion (N/50mm) and d2: Tensile strength (MPa)).

To choose the best coordinates of the acceptable compromise, we take into account the economic and process aspects of the mixture preparation. Thus, the acceptable compromise is selected at the point: $X_T=190^\circ\text{C}$ and $X_{PE}=29\%$ giving an interfacial adhesion of 28N/50mm and a tensile strength which reaches a value of 24 MPa. The choice has been made in the purpose of promoting the flexibility and the fuel resistance properties of the material. The LDPE has poor fuel resistance properties so it is necessary to have a material with a major part of TPU.

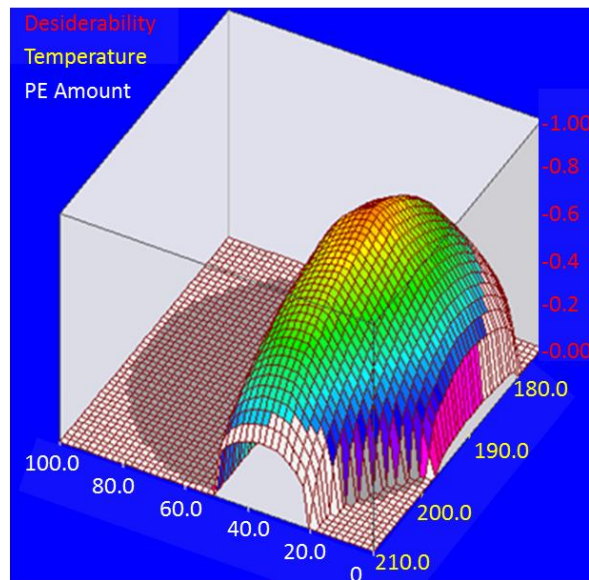


Figure 8: Response surface of the global desirability function.

Thanks to the experimental design, we have chosen the composition and the extrusion temperature to have the highest value of peel strength but also a high value of tensile strength (>22MPa). However the value of tensile strength of the blend for the chosen extrusion temperature was still lower than that of the 2 components due to the incompatibility of TPU and LDPE (38). For the next part of our study, we added 3 other compositions with maleic anhydride which is a compatibiliser for these blends (37). The LLDPE-g-Ma was not used in the first part of the study because of the important price of it compared to the price of LDPE. The blend 13 was composed of 71%wt TPU and 29%wt of LLDPE-g-Ma. We substituted the LDPE by LLDPE-g-Ma to check its influence on the peel strength. The blend 14 was composed of 71%wt of TPU, 26%wt of LDPE and 3%wt of LLDPE-g-Ma. The purpose of this blend was to get a blend similar to the best one determined before with the addition of 3% of Ma to increase the tensile strength. Then the experiment 15 was the neat LLDPE-g-Ma which was a reference like experiments 10, 11 and 12.

The peel strength and tensile strength of experiments 13, 14 and 15 are summarized in the Table XIII.

Table XIII: Peel strength and tensile strength of experiments 13, 14 and 15

Sample number	13	14	15
---------------	----	----	----

Amount of LDPE (%)	0	26	0
Amount of LLDPE-g-Ma	29	3	100
Die temperature (°C)	190	190	175
Peel strength (N/50mm)	16.5	30.7	4.8
Standard deviation	1.87	3.09	0.7
Tensile Strength (MPa)	31.5	26.51	27.12
Standard deviation	1.26	0.3	1.35

3.4 Analysis of the compatibility TPU/LDPE, TPU/LLDPe-g-Ma and

TPU/LDPE/LLDPE-g-Ma

The analysis of the film surface of the blends shows three different morphologies: nodular, co-continuous and continuous (Figure 9). For all the LDPE/TPU blends (experiments 1 to 9), the morphology is nodular (Figure 9.A) which is a proof of the immiscibility of the LDPE in TPU. Also the smooth interface between the 2 components indicates that there is a poor interfacial adhesion. A co-continuous morphology was observed for LDPE/LLDPE-g-Ma/TPU (experiment 14) (Figure 9.B) and almost continuous for LLDPE-g-Ma/TPU blend (experiment 13) (Figure 9.C) which means that there is a better miscibility between TPU and LLDPE-g-Ma. As said previously in the introduction, the g-Ma is a compatibiliser for LDPE and TPU so these results are in agreement with the literature (36). On the pictures it is clear that the polymer is oriented in one direction. This is due to the process and especially to the rolls of the calendering unit.

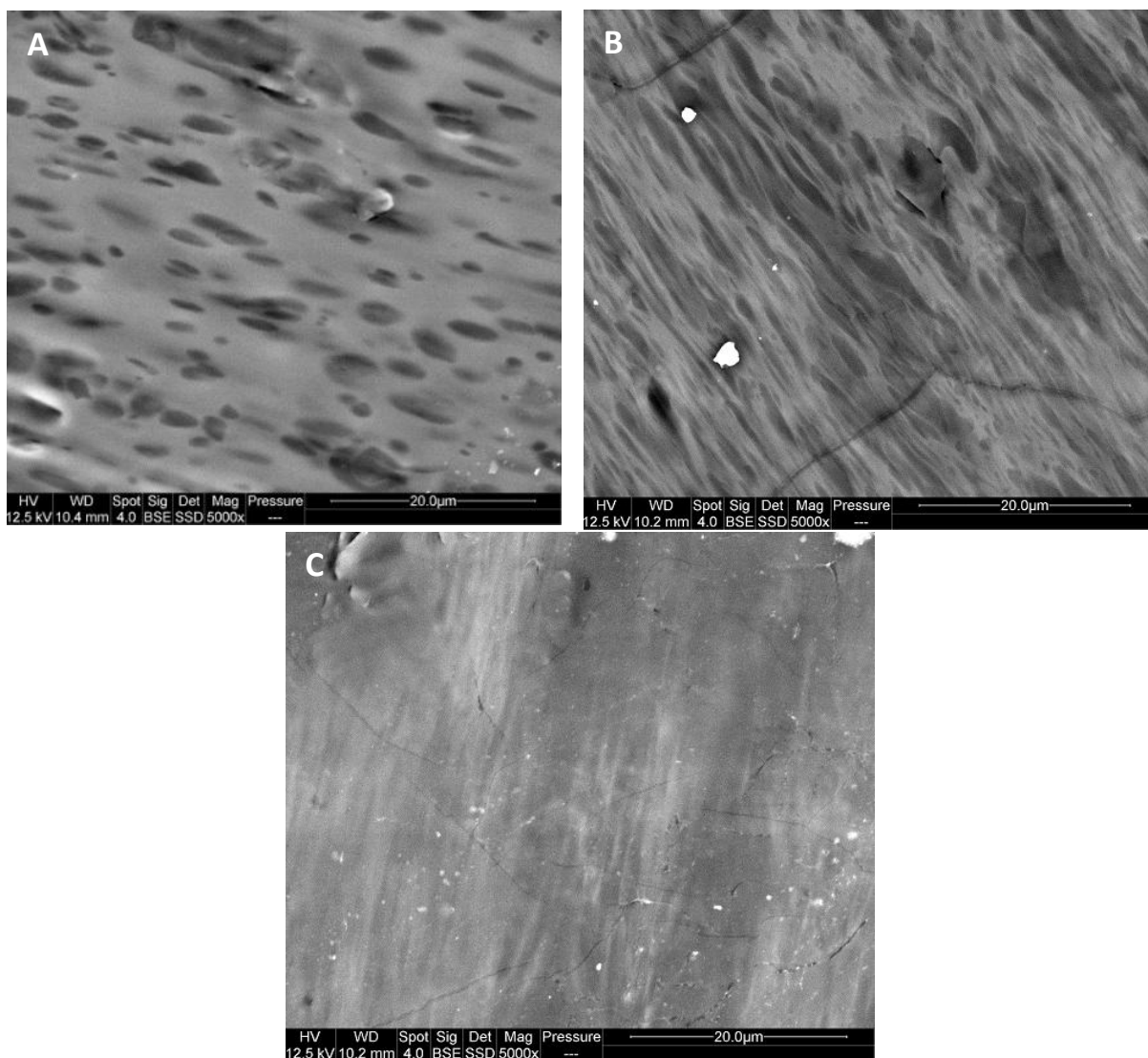


Figure 9: SEM pictures of the film morphologies for: A: nodular (experiment 5), B :co-continuous (experiment 14), C: continous (experiment 13).

3.5 Analysis of the chemical composition

FTIR Spectrum of neat LDPE and neat LLDPE-g-Ma are very similar (Figure 10). The Ma group can be seen around 1700 cm^{-1} and 1800 cm^{-1} (Figure 11) as explained on previous research for PP-g-Ma (48) (49) and EPDM (50). Figure 12 shows the FTIR spectrum of experiment 2 and 6. Although the peel strength is very different (sample 6 displayed a peel strength almost 3 times higher than sample 2), the 2 spectrum are similar. No difference was observed on the FTIR spectrums of the blends 1 to 9. The FTIR spectrums of experiment 6, 13 and 14 are presented in Figure 12 and 13 and the same conclusion can be made. The percentage of Ma in the blends 13 and 14 is so weak that it is almost not visible on the FTIR experiment except for the peak around 1730cm^{-1} as it can be seen on the Figure 13. The large

peak around 1700 cm^{-1} is a peak from TPU corresponding to the urethane group ($\text{C}=\text{O}$) (51) and cannot be attributed to Ma.

In conclusion to these analyses, no significant difference on the FTIR spectrum has been observed between all the blends. It means that there is no new-bonds creation by mixing TPU and LLDPE or LLDPE-g-Ma so the noted better adhesion is not due to a chemical link between the fabric and the coating.

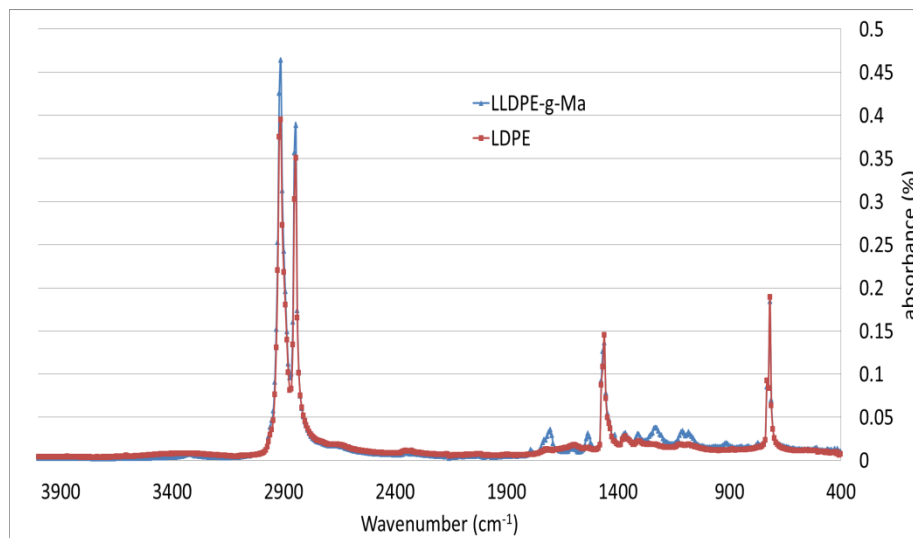


Figure 10: FTIR spectrum of neat LDPE and neat LLDPE-g-Ma.

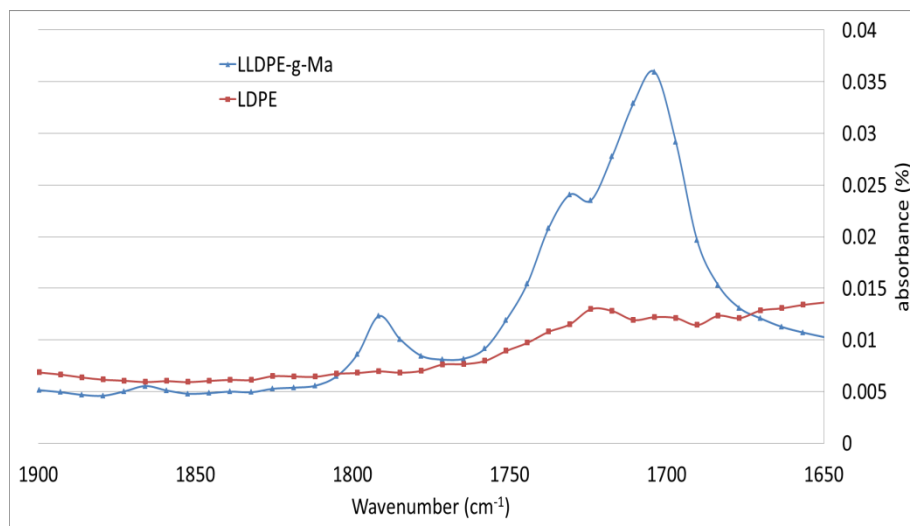


Figure 11: FTIR spectrum ($1650\text{-}1900\text{cm}^{-1}$) of neat LDPE and neat LLDPE-g-Ma.

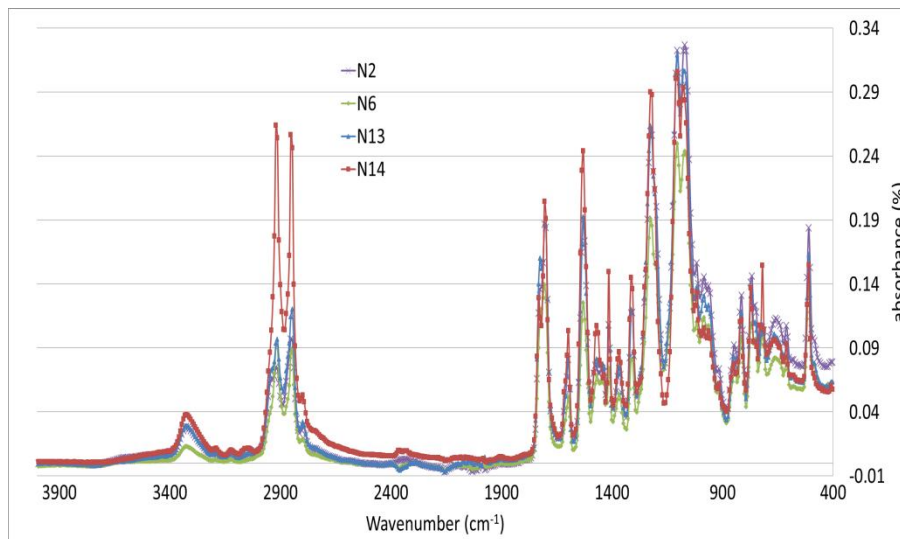


Figure 12: FTIR spectrum of experiment 2, 6, 13 and 14.

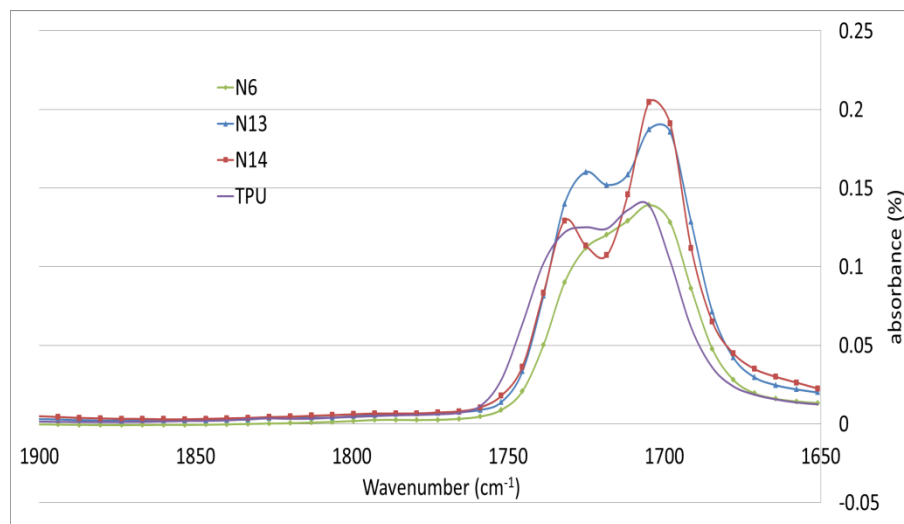


Figure 13: FTIR spectrum (1650-1900cm⁻¹) of neat TPU and experiment 6, 13 and 14.

3.6 Analysis of the shear viscosity of the blend

The viscosity of the sheet is important because the ability of the polymer to penetrate inside the yarn depends of this viscosity. The shear viscosity given in the Table XIV is the viscosity of the different blends at the corresponding extrusion temperatures for a shear rate between 10 s⁻¹ and 100 s⁻¹. These shear rates are those corresponding to the calendering process according to the literature (52) (53) (54).

Table XIV: Shear rate viscosities of neat TPU, neat LDPE, neat LLDPE-g-Ma and of the different blends at the corresponding processing temperatures and for a shear rate between 10s⁻¹ and 100s⁻¹.

Sample number	1	2	3	4	5	6	7	8	9	10	11	12	13	14	15
---------------	---	---	---	---	---	---	---	---	---	----	----	----	----	----	----

Amount of LDPE (%)	16.6	19	19	22.5	15	29	22.5	16.6	15	0	100	100	0	26	0
Amount of LLDPE-g-Ma (%)	0	0	0	0	0	0	0	0	0	0	0	0	29	3	100
Die temperature (°C)	199	174	196	190	196	190	210	181	174	175	174	190	190	190	175
Shear rate viscosity (Pa.s) $10s^{-1} - 100s^{-1}$	110 93	481 284	119 96	222 166	112 99	421 267	47 43	447 276	487 335	237 188	3800 960	2900 700	445 248	884 485	2980 1300

At the same die temperature, the viscosity of neat LDPE and neat LLDPE-g-Ma is 7 times higher than the viscosity of neat TPU. Although the viscosity of LLDPE-g-Ma is lower than LDPE ones, the blend of LLDPE-g-Ma/LDPE/TPU (experiment 14) has a viscosity twice higher than that of experiment 6 for a same temperature of process. This must be linked with the miscibility of the different materials and it should be compared with the mechanical performance and the morphology of the blends. For the same LDPE/TPU blends, the higher the process temperature is, the lower is the viscosity. For example for an amount of 22.5% wt of LDPE and a shear rate of $10s^{-1}$, the viscosity is about 421 Pa.s for a temperature of $190^{\circ}C$ and 47 Pa.s for a temperature of $210^{\circ}C$.

3.7 Analysis of the coated textile sections

The analysis of the coated textile section gives important information about the depth of penetration of the polymer between the filaments of the yarns that compose the fabric. The Table XV gives the depth of penetration for each experiment. The coating has a better penetration when extruded at high temperature especially if the temperature is higher than $190^{\circ}C$. It could be due to a difference of surface energy or viscosity. However it is important to notice that the diameter of a filament is $23 \mu m$ so the coating never penetrates inside the fabric but always keeps on the surface (Figure 14).

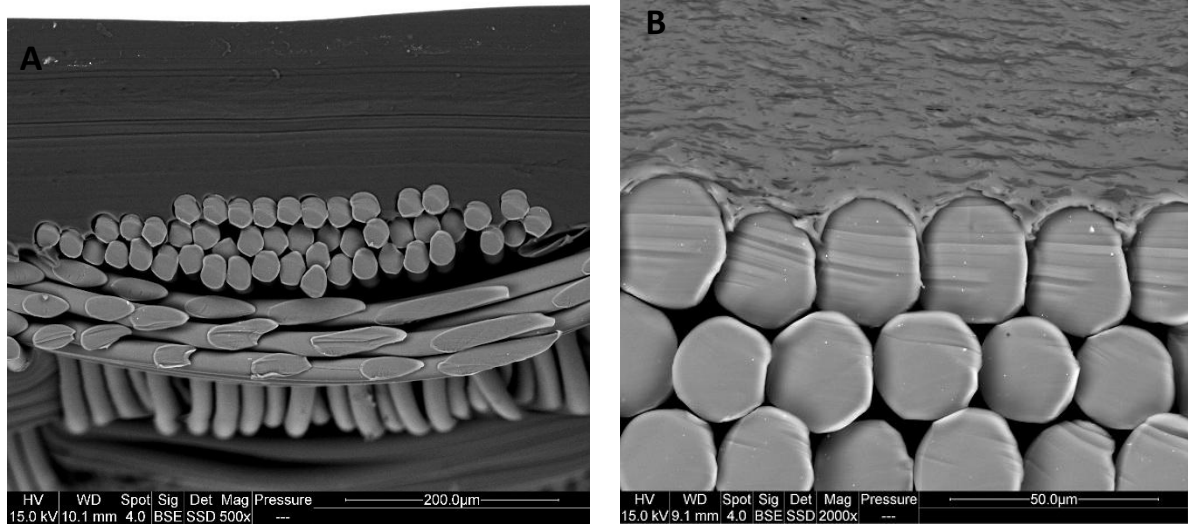


Figure 14: sections of the coated textile: A: experiment 11 and B: experiment 7.

Table XV: Penetration depth of the coating for each blend in the fabric.

Sample number	1	2	3	4	5	6	7	8	9	10	11	12	13	14	15
Amount of LDPE (%)	16.6	19	19	22.5	15	29	22.5	16.6	15	0	100	100	0	26	0
Amount of LLDPE-g-Ma (%)	0	0	0	0	0	0	0	0	0	0	0	0	29	3	100
Die temperature (°C)	199	174	196	190	196	190	210	181	174	175	174	190	190	190	175
Penetration depth (μm)	13	6	11	10	9	7	14	8	7	2	5	6	8	6	2

4. Discussion

4.1 Analysis of the peel strength increase

According to the literature, the coating peel strength on a substrate is directly related to the six adhesion theories mentioned in introduction. However for this case, the theories of the weak boundary layer, electrostatic and diffusion cannot be used to explain the results.

FTIR shows that no new chemical bonds have been created in any of the different blends. Indeed, despite the large difference of peel strength, all the FTIR spectrums are identical. It

means that the peel strength difference is not due to the creation of a new chemical bond between the fabric and the coating.

Regarding the theories of wetting and mechanical interlocking, the observations of the coating penetration depth in the fabric give good information. As expected, the lower is the viscosity, the better is the penetration. According to the results, peel strength seemed to increase when coating penetration was higher than $7\mu\text{m}$. For example, on sample 7, the penetration is about $14\mu\text{m}$ and the peel strength is $21.2\text{ N}/50\text{mm}$ while penetration is only $2\mu\text{m}$ for sample 10 and the corresponding peel strength $1.8\text{ N}/50\text{mm}$. But this trend could not be generalized; in fact sample 6 displayed a $30\text{ N}/50\text{ mm}$ peel strength with a penetration depth of only $7\mu\text{m}$. The conclusion is that the coating penetration depth in the fabric, and the related viscosity, has a strong influence on the peel strength but is not the only parameter involved.

Actually, the temperature seems to have a strong impact on the peel strength. The temperature dependence of surface energy has been shown by previous papers (55) (56) (57). This modification of surface energy could lead to a better affinity between the fabric and the coating. As said previously, for a same amount of LDPE an increase of the extrusion temperature leads to an increase of the peel strength until a maximum value for a temperature of 190°C . For higher temperatures (experiment 1, 3, 5 and 7), the peel strength decreases as a consequence of the polymer degradation, which could be observed by the decrease of the tensile strength.

The low significance value obtained with the experimental design means that there is a good correlation between the model and the experiments. The experimental design also allows us to determine the best coating composition and the best extrusion temperature to get the highest possible value of peel strength and a good value of tensile strength.

4.2 Maleic anhydride influence analysis

As observed previously, the complete substitution of LDPE by LLDPE-g-Ma has a negative impact on the peel strength, but a substitution of only 3%wt of LDPE by LLDPE-g-Ma did not degrade this property while it increases its tensile strength. The LLDPE-g-Ma is needed to get good peel strength and also good tensile properties.

Actually, the addition of maleic anhydride in the blend created a modification of the initial nodular morphology to a co-continuous morphology for blends with 3%wt of Ma and to almost continuous morphology for blends with 29%wt of Ma. This is in perfect accordance with the literature (36) (37) (38). Other tests like tear strength or measurements of interfacial tensions using the Palierne's model have been performed on the blends. The results will be published soon in another paper. The interfacial decreases significantly with the addition of **maleic anhydride**. This is a proof of the compatibilisation of the blend. One interesting point is the difference of viscosity between experiment 6, 13 and 14 which have the same amount of LDPE or LLDPE-g-Ma. At the same temperature, LLDPE-g-Ma has a lower viscosity than LDPE. But also for a same temperature, the viscosity of the blend 14 made of 26%wt of LDPE and 3%wt of LLDPE-g-Ma is 2 times higher than the viscosity of the blend 6 made with 29%wt of LDPE and blend 13 with 29%wt of LLDPE-g-Ma. This increase of viscosity means that there is a good compatibility between LDPE and LLDPE-g-Ma. The complete substitution of LDPE by LLDPE-g-Ma seems to not have any impact on the viscosity of the blend at 190°C as it was found by comparing experiment 6 and 13.

5. Conclusion

In the present paper, the impact on peel strength of the addition of low density polyethylene and linear low density polyethylene to a thermoplastic polyurethane sheet calendered on a polyester fabric has been studied. This study has been divided into two parts.

In the first part, the study has shown that the addition of LDPE in the TPU coating has no direct impact on the peel strength while the die temperature has a strong influence. It has been

shown that an increase of the extrusion temperature leads to an increase of the peel strength. However it is important to note that the best peel strength is obtained for an extrusion temperature of 190°C which is not the highest temperature. This must be due to a degradation of the film at higher temperature as shown by analyzing the tensile strength. The increase of the peel strength can be attributed to several phenomena among which the penetration of the coating in the fabric which creates a mechanical interlocking, and the extrusion temperature which create a different surface energy of the coating resulting in a better affinity with the fabric. This theory will have to be proved for our study in a future work by using a pendant drop experiment as previously realized by Kwok et al (58).

In a second part, the influence of maleic anhydride as a compatibiliser between TPU and LDPE has been studied with the addition of LLDPE-g-Ma. It has been shown that the substitution of LDPE by LLDPE-g-Ma has a negative impact on the peel strength but hugely increases the tensile strength. However the substitution of only 3%wt of LDPE (among 29%wt) by LLDPE-g-Ma has no impact on the peel strength but still increases the tensile strength.

In future work, this experimental investigation will be continued firstly with a study of the extruded coating sheet surface energy depending on the die temperature. The effect of the temperature on the surface energy will be helpful to confirm the theory proposed in our conclusion to explain the better adhesion. Also it will be important to focus on **the** other kind of bonds among polymers and interfaces to explain the better adhesion.

References

1. **Akovali, G.** *Toxicity of Building Materials: 2 – Plastic materials: polyvinyl chloride (PVC)*. s.l. : Woodhead Publishing Series in Civil and Structural Engineering, 2012. pp. 23-53.
2. **Koch, H-J.** *The Structure and Properties of Polyurethane Textile Coating*. s.l. : Journal Coated Fibrous Materials, 1971. Vol1 p118.
3. **H.Wang, Y. Wang, D. Liu, Z. Sun and H. Wang.** *Effects of Additives on Weather-Resistance Properties of Polyurethane Films Exposed to Ultraviolet Radiation and Ozone Atmosphere*. s.l. : Journal of Nanomaterials, 2014. Vol. 2014. Vol 2014, ID 487343.
4. **D.J. Mills, S.S. Jamali, K. Paprocka.** *Investigation into the effect of nano-silica on the protective properties of polyurethane coating*. s.l. : Surface and Coatings Technology, 2012. Vol 209, pp 137-142.
5. **E.A. Papaj, D.J. Mills, S.S. Jamali.** *Effect of hardener variation on protective properties of polyurethane coating*. s.l. : Progress in Organic Coatings, 2014. vol 77, pp 2086-2090.
6. **V.V. Gite, P.P. Mahulikar, D.G. Hundiwale.** *Preparation and properties of polyurethane coatings based on acrylic polyols and trimer of isophorone diisocyanate*. s.l. : Progress in Organic Coatings, 2010. Vol 307, pp 307-312.
7. **J. Zhang, C. Pu Hu.** *Synthesis, characterization and mechanical properties of polyester-based aliphatic polyurethane elastomers containing hyperbranched polyester segments*. s.l. : European Polymer Journal, 2008. Vol 44, pp 3708-3714.
8. **S-Y Moon, Y-D Park, C-J Kim, C-H Won, and Y-S Lee.** *Effect of Chain Extenders on Polyurethanes Containing Both Poly(butylene succinate) and Poly(ethylene glycol) as Soft Segments*. s.l. : Bull. Korean Chem. Soc., 2003. Vol. 24, pp 1361-1364.
9. **R.W.Oertel, R.P. Brentin.** *Thermoplastic Polyurethane for Coated Fabrics*. s.l. : Journal of Coated Fabrics, 1992. 0093-4658/92/02 0150-11.
10. **Schmelzer, H. G.** *Polyurethanes for Flexible Surface Coatings and Adhesives*. s.l. : Journal of coated fabrics, 1988. 0093-4658/88/03 0167-16.
11. **A. Euler, H. Zhai.** *Material Challenges for Lighter-Than-Air Systems in High Altitude Applications*. s.l. : AIAA 5th Aviation, Technology, Integration, and Operations Conference, 2005. AIAA 2005-7488.
12. **Singa, K.** *A Review on Coating & Lamination in Textiles: Processes and Applications*. s.l. : American Journal of Polymer Science, 2012. Vol 2, pp 39-49.
13. **Lee, Stuart M.** *Dictionary of Composite Materials Technology*. s.l. : Taylor and Francis, 1995. ISBN-10: 0877626006 .
14. **J.W. McBain, D.G. Hopkins.** *On adhesive and adhesive action*. s.l. : The Journal Of Physic Chemistry, 1925. Vol 29, pp 188-204.
15. **H. Schonborn, L.H. Sharpe.** *Surface tension of molten polypropylene*. 1963. p 15-63.
16. **Voyutskii, S.S.** *Autoadhesion and adhesion of high polymers*. s.l. : Wiley-Interscience and Sons: New-York, 1963. p 405.

17. **B.V Deryagin, Y. Toprov.** *Role of the molecular and electrostatic force in the adhesion of polymers.* 1983. p 605-626.
18. **S.Buchan, W.D.Rae.** *Chemical nature of the rubber to glass bond.* s.l. : Trans. Inst. Rubber Industry, 1946. Vol 20, pp 205-216.
19. **Bikerman, J.J.** *The Science of Adhesive Joints.* s.l. : ACADEMIC PRESS, New-York and London, 1961.
20. **Mittal, K.L.** *The Role Of The Interface In Adhesion Phenomena.* s.l. : Polymer Engineering and Science, 1977. Vol 17, pp 467-473.
21. **J.Schultz, L.Lavielle, C.Martin.** *The Role of the Interface in Carbon Fibre-Epoxy Composites.* s.l. : The Journal of Adhesion, 1987. Vol23, pp 45-60.
22. **F. Leroux, C. Campagne, A. Perwuelz, L. Gengembre.** *Atmospheric air plasma treatment of polyester textile materials. Textile structure influence on surface oxidation and silicon resin adhesion.* s.l. : Surface & Coatings Technology, 2009. Vol 203, pp 3178-3183.
23. **M.N. Belgacem, A. Gandini.** *Surface Modification of Cellulose Fibres.* s.l. : Polímeros: Ciência e Tecnologia, 2005. vol. 15, pp 114-121.
24. **C.W. Kan, C.W.M. Yuen.** *Effect of atmospheric pressure plasma treatment on wettability and dryability of synthetic textile fibres.* s.l. : Surface & Coatings Technology, 2011. Vol 228, pp S607–S610.
25. **S. Garg, C. Hurren, A. Kaynakc.** *Improvement of adhesion of conductive polypyrrole coating on wool and polyester fabrics using atmospheric plasma treatment.* s.l. : Synthetic Metals, 2007. Vol 151, pp 41-47.
26. **T. Oktem, N. Seventekin, H. Ayhan, E. Piskin.** *Modification of Polyester and Polyamide Fabrics by different in-situ Plasma Polymerization Methods.* s.l. : Turkey Journal Chemistry, 1999. Vol 24, pp 275-285.
27. **J. Yip, K. Chan, K.M. Si, K.S. Lau.** *Surface Modification of Polyamides Materials With Low Temperature Plasma.* s.l. : Research Journal Of Textile and Apparel, 2001. Vol 5, pp10-18.
28. **R. Morent, N. De Geyter, J. Verschuren, K. De Clerck, P. Kiekens, C. Leys.** *Non-thermal plasma treatment of textiles.* s.l. : Surface and Coatings Technology, 2007. Vol 202, pp 3427–3449.
29. **Ferrero, F.** *Wettability measurements on plasma treated synthetic fabrics.* s.l. : Polymer Testing, 2002. Vol 22, pp 571–578.
30. **I. Novak, S. Florian.** *Investigation of long-term hydrophobic recovery of plasma modified polypropylene.* s.l. : Journal of Materials Science, 2004. Vol 29, pp 2033–2036.
31. **M. N. Belgacem, P. Bataille, and S. Sapiaha.** *Effect of Corona Modification on the Mechanical Properties of Polypropylene/ Cellulose Composites.* s.l. : Journal of Applied Polymer Science, 1994. Vol 53, pp 379–385.
32. **Ragoubi, M.** *Contribution à l'amélioration de la compatibilité interfaciale fibres naturelles/matrice thermoplastique via un traitement sous décharge couronne.* 2010.

33. **M. Ragoubi, D. Bienaimé, S. Molina, B. Georgea, A. Merlina.** *Impact of corona treated hemp fibres onto mechanical properties of polypropylene composites made thereof.* s.l. : Industrial Crops and Products, 2009. Vol 31, pp 344–349.
34. **A.K. Bledzki, J. Gassan.** *Composites reinforced with cellulose based fibres.* s.l. : Progress in Polymer Science, 1999. Vol 24, pp 221–274.
35. **J. ZL, W. Qinglin, S. Harold.** *Chemical coupling in wood fibre and polymer Composites: A review of coupling agents and treatments.* s.l. : Wood and fibre Science, 2000. Vol 32, pp 88-104.
36. **P.Potschke, K.Wallheinke.** *Blends of Thermoplastic Polyurethane and Maleic- Anhydride Grafted Polyethylene .* s.l. : POLYMER ENGINEERING AND SCIENCE, 1999. Vol. 39, pp 1035-1048.
37. **J. Song, R.H. Ewoldt, W. Hu, H.C. Silvis, C.W. Macosko.** *Flow Accelerates Adhesion Between Functional Polyethylene and Polyurethane.* s.l. : American Institute of Chemical Engineers, 2011. Vol 57, pp 3496–3506.
38. **J. Song, A. Batra, J.M. Rego, C.W. Macosko.** *Polyethylene/polyurethane blends for improved paint adhesion.* s.l. : Progress in Organic Coatings, 2011. Vol 72,pp 492–497.
39. **Y. Luo, Y. Zhao, Y. Duan, S.D. School.** *Surface and wettability property analysis of CCF300 carbon fiber with different sizing or without sizing.* s.l. : Materials and Design, 2011. Vol 32, pp 941–946.
40. **M.Roosta, M.Ghaedi, A.Daneshfar, S.Darafarin, R.Sahraei, M.K. Purkait.** *Simultaneous ultrasound-assisted removal of sunset yellow and erythrosine by ZnS:Ni nanoparticles loaded on activated carbon: Optimization by central composite design.* s.l. : Ultrasonics Sonochemistry, July 2014. Vol 21, pp 1441-1450.
41. **A.I.C. Gonçalves, L.A. Rocha, J.M.L. Dias, L.A. Passarinha, A.S Sousa.** *Optimization of a chromatographic stationary phase based on gellan gum using central composite design.* s.l. : Journal of Chromatography B, April 2014. Vol 957, pp 46-52.
42. **J. Sanz, M. Pérez, M.T. Martinez, M. Plaza.** *Optimization of dimethyltin chloride determination by hydride generation gas phase molecular absorption spectrometry using a central design composite design.* s.l. : Talanta, April 2000. Vol 51, pp 849-862.
43. **G.A. Lewis, D. Mathieu, R. Phan-Tan-Luu.** *Pharmaceutical Experimental Design.* s.l. : Marcel Dekker, 1999. ISBN 9780824798604.
44. **Goupy, J.** *Plans d'Experiences Pour Surfaces de Réponse.* Paris : Dunod, 1999. EAN : 9782100039937 .
45. **R.H. Myers, D.C. Montgomery.** *Response Surface Methodology: Process and Product Optimization Using Design Experiments.* New-York : Wiley, 1995. ISBN: 978-0-470-17446-3.
46. **D. Mathieu, R. Phan-Tan-Luu.** *Plans d'experiences: Application à l'entreprise.* Paris : Technip, 1997. ISBN : 9782710807339.
47. **sscrew.** *Polymer processing.* [Online] 2001.
<http://www.polymerprocessing.com/operations/sscrew/big.html>.

48. **A. Oromiehie, H. Ebadi-Dehaghani, S. Mirbagheri.** *Chemical Modification of Polypropylene by Maleic Anhydride: Melt Grafting, Characterization and Mechanism.* s.l. : International Journal of Chemical Engineering and Applications, 2014. Vol 5, pp 117-122.
49. **B. De Roover, M. Sclavons, V. Carlier, J. Devaux, R. Legras, and A. Momtaz.** *Molecular Characterization of Maleic Anhydride-Functionalized Polypropylene.* s.l. : Journal of Polymer Science: Part A: Polymer Chemistry, 1995. Vol 33, pp 829–842.
50. **G.M.O. Barra, J.S. Crespo, J.R. Bertolino, V. Soldi, A.T. Nunes Pires.** *Maleic Anhydride Grafting on EPDM: Qualitative and Quantitative Determination.* s.l. : Journal of the Brazilian Chemical Society, 1999. Vol 10, pp 31-34.
51. **N. Liu, Y.Zhao, M. Kang, J. Wang, X. Wang, Y. Feng, N. Yin, Q. Li.** *The effects of the molecular weight and structure of polycarbonatediols on the properties of waterborne polyurethanes.* s.l. : Progress in Organic Coatings, 2015. Vol 82, pp 46-56.
52. **M-C. Serrat, J-F. Agassant, J. Bikard, S. Devisme.** *Influence of the calendering step on the adhesion properties of coextruded structures.* s.l. : international Polymer Processing, 2012. Vol 27, pp 318-327.
53. **Nass, Leonard I.** *Encyclopedia of PVC, Second Edition, Revised and Expanded.* s.l. : CRC PRESS, 1992. ISBN-10: 082477695X.
54. **Cheremisinoff, N.P.** *Polymer mixing and extrusion technology.* s.l. : Marcel Dekker Inc, 1987. ISBN 9780824777937.
55. **J.D. Bernardin, I. Mudawar, C.B. Walsh, E.I. Franses.** *Contact angle temperature dependence for water droplets on practical aluminium surfaces.* s.l. : International Journal Heat Mass Transfer., 1996. Vol 40, pp 1017-1033.
56. **H. Matsuoka, K. Oka, Y. Yamashita, F. Saeki, S. Fukui.** *Deformation characteristics of ultra-thin liquid film considering temperature and film thickness dependence of surface tension.* s.l. : Microsyst technol, 2011. Vol 17, pp 983–990.
57. **L.H. Blanco, O.M. Vargas, A.F. Suarez.** *Effect of temperature on the density and surface tension of aqueous solutions of HMT.* s.l. : Journal of Thermal Analysis and Calorimetry, 2011. Vol 104, pp 101–104.
58. **D.Y.Kwok, L.K. Cheung, C.B.Park, A.W. Neumann.** *Study on the surface tensions of polymer melts using axisymmetric drop shape analysis.* s.l. : Polymer Engineering and Science, 1998. Vol 38, pp 757-764.